

Supplementary Information for

Effect of salt on the formation of salt-bridges in β -hairpin peptides

By Shahar Sukenik, Yoav Boyarski and Daniel Harries

1. Materials

All peptides used in this study (K1, seq: AcKK(Ac)YTVSINGKKITVSI; K2, seq: AcK(Ac)KYTVSINGKKITVSI; and K1K2 seq: AcKKYTVSINGKKITVSI) at > 95% purity were purchased from GL Biochem (Shanghai, China) and used without further purification. Purity was independently assessed using analytical HPLC (Merck-Hitachi with a C8 column, run in a 5-60% acetonitril gradient over 25 minutes) and MALDI-TOF mass-spectrometry (Applied Biosystems), as shown in Figure S1. Sodium Chloride (NaCl) was purchased from Sigma, and used without further purification. All samples contained 10mM phosphate buffer, at pH 7 or 2, as specified.

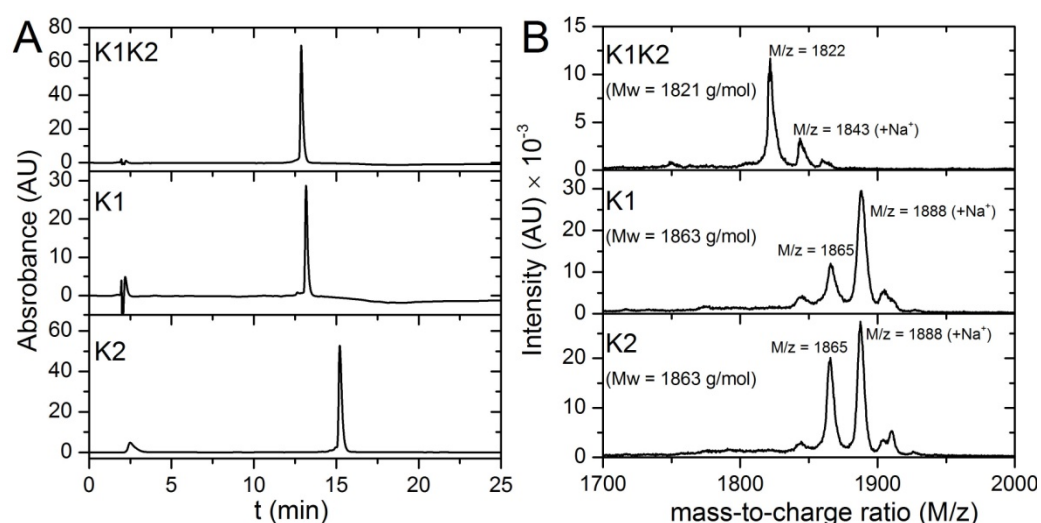


Figure S1. Peptide purity determination. (A) Analytical HPLC chromatograms show all peptides to be > 95% pure. (B) MALDI-TOF mass-spectroscopy show correct mass-to-charge ratios for all peptide homologues. Theoretical mass appears in parentheses on the left of each panel.

2. Experimental procedures

a. Circular dichroism measurements

Circular dichroism (CD) measurements were conducted on a Jasco J-810 spectrometer (Jasco, Japan). For each experiment, the appropriate homologue peptide was dissolved in water, and the concentration tested using Tyr absorbance (Nano-drop, Thermo scientific). After buffer addition, pH was

verified (Accumet Basic, Fischer Scientific) and the sample was placed in a 2mm quartz cuvette (Starna), allowed to thermally equilibrate, and measured. Unless otherwise stated, measurements were at 298K. For each spectrum, five scans were acquired over the 190-260 nm wavelength range and averaged. Salt titrations were performed using a concentrated NaCl stock filtered with a 0.2 μm filter. The cuvette was inverted 5-10 times after each titration to allow proper mixing. The resulting ellipticity spectra were baseline-corrected by subtracting the signal in the absence of peptide. All spectra were normalized to a peptide concentration of 100 μM using Tyr absorption or normalized to a spectrum of the same concentration using a Matlab least-square minimization procedure. Once normalized, all peptides under all conditions displayed an isodichroic point at $\lambda = 208 \pm 1$ nm (shown in Figs. S3-S5). The fully folded states were determined using a 1:1 volume water-methanol solution, and showed a minimum of $\theta = -30.0$ mdeg at $\lambda = 215$ nm at a peptide concentration of 100 μM at 278K. The fully unfolded ensemble has previously been shown to possess a value of $\theta = 0$ at the same wavelength and concentration.¹⁻³ Additional details on analysis are available in Section 3a. The experimental values for ellipticities used to calculate ΔG values for all homologues reported are shown in Table S1.

Table S1. Ellipticity values for NaCl titration in all peptide homologues and conditions at 100 μM concentration.

K1K2 pH 7		K1 pH 7		K2 pH 7		K1K2 pH 2		K1 pH 2		K2 pH 2	
[NaCl] ^a	θ_{215} ^b	[NaCl] ^a	θ_{215} ^b	[NaCl] ^a	θ_{215} ^b	[NaCl] ^a	θ_{215} ^b	[NaCl] ^a	θ_{215} ^b	[NaCl] ^a	θ_{215} ^b
0	-18.3	0	-18.3	0	-16.8	0	-18.3	0.000	-18.3	0.000	-16.8
0.005	-18.4	0.015	-17.6	0.005	-16.6	0.004	-18.2	0.005	-18.2	0.007	-16.7
0.007	-18.3	0.030	-18.0	0.020	-16.8	0.020	-18.4	0.020	-18.3	0.015	-16.8
0.013	-17.8	0.038	-17.4	0.043	-17.3	0.029	-18.4	0.043	-18.6	0.030	-16.7
0.020	-18.3	0.078	-17.7	0.049	-16.2	0.039	-18.1	0.087	-18.6	0.038	-17.0
0.022	-18.6	0.087	-17.4	0.078	-16.2	0.042	-18.5	0.163	-18.9	0.078	-16.8
0.039	-18	0.163	-17.3	0.087	-17.1	0.058	-18.4	0.308	-18.9	0.087	-16.9
0.043	-18.2	0.172	-17.5	0.098	-16.6	0.072	-18.6	0.486	-18.8	0.163	-17.3
0.054	-17.6	0.308	-16.5	0.163	-17.7	0.086	-18.5			0.172	-16.7
0.072	-18	0.347	-16.9	0.172	-16.5	0.121	-18.4			0.308	-17.6
0.087	-17.9	0.486	-16.3	0.190	-16.4	0.142	-18.7			0.347	-17.2
0.121	-17.8	0.653	-17.3	0.308	-17.5	0.205	-18.9			0.486	-18.2
0.158	-17.5	1.026	-17.3	0.347	-16.3	0.273	-18.7			0.653	-17.7
0.182	-17.4	1.492	-17.3	0.404	-16.6	0.319	-19.0			1.026	-18.5
0.310	-16.9			0.486	-16.3	0.326	-19.0				
0.410	-17			0.653	-16.6	0.451	-19.5				
0.486	-16.5			0.768	-17.2	0.553	-19.2				
0.803	-17.1			1.193	-18	0.887	-19.7				
1.104	-16.9			1.232	-16.8	0.972	-19.6				
1.358	-17			1.612	-18.5	1.173	-19.8				
1.575	-17.4			1.943	-18.7						
1.927	-17.4										
2.072	-17.6										
2.201	-17.6										

^a in mol/L; ^b in mdeg

b. Temperature dependent measurements

Temperature dependence of peptide stability was measured using a Jasco J023A Peltier device to control the temperature of sample cells. Ellipticities of peptide solution were scanned at $\lambda = 215$ nm from 278 to 333 K in 5 K increments, with 5 minutes wait-time before each scan to assure thermal equilibration. Full scans over the $\lambda = 190 - 260$ nm range were performed at 278 K, 298 K, and 333 K to test for the isodichroic point, then again at 298 K to ensure that folding is completely reversible over the temperature range studied.

3. Data analysis

a. Determining the baseline of fully folded and unfolded peptides

In previous works, the K1K2 peptide was used and the fully folded (β -hairpin) and fully unfolded spectra, representative of the two states, were determined. Searle and co-workers, who first synthesized this peptide, observed and characterized in depth its two-state folding using both NMR and CD spectroscopy.^{1,2,4} Specifically, Searle *et al.* characterized the folding process using NMR by comparing the root-mean-square deviation (RMSD) of the $H\alpha$ chemical shifts to known random-coil values.^{5,1} This method was then used to determine the extent of folding of the peptide, where the fully unfolded peptide has an RMSD of 0. The unfolded values of $H\alpha$ were also tested by calculating the RMSD of the $H\alpha$ shifts of the K1K2 peptide from those of a single strand (residues 9-16) of the peptide, which is unable to fold to a hairpin. Both comparisons yielded very similar results.

For the fully folded spectrum, the RMSD value obtained by Searle and co-workers showed a maximum at 50% (v/v) methanol solution, at 278 K. Heating the solution caused the folded population to decrease. Therefore, we also used these conditions in our work to promote full folding of the peptides.

In this work, the limiting fully-folded CD signal value at $\lambda = 215$ nm was determined as $\theta_{215} = -30$ mdeg from 100 μ M peptide in 50% (v/v) methanol solution at 278K. To test that these conditions indeed cause full folding of the peptide, we followed changes in the minimum at $\lambda = 215$ nm upon heating, as shown in Fig. S2. In line with Searle's observation,^{4,1} we observed a decrease in the value, that reaches a plateau below $T = 280$ K.

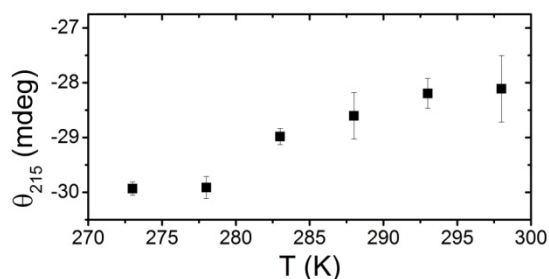


Figure S2. Temperature variance of CD signal at $\lambda = 215$ nm in the presence of 50% (w/w) methanol in the K1K2 peptide. The curve shows the signal reaches a limiting value at low temperatures, indicating a fully folded population. Error bars are standard deviations from 3 repeats.

The limiting fully-unfolded CD signal at 215 nm ($\theta = 0$) was compared by Searle¹ with a CD spectrum of a characteristic random-coil (PPII) conformation, which displays an ellipticity of $\theta_{215} = 0$ mdeg. We further verified this value by extending the stabilization and destabilization range of the peptide with titration of the peptide with trehalose in the presence and absence of guanidinium hydrochloride (GuHCl).³ Whereas GuHCl is a denaturant, and is expected to shift population towards the unfolded ensemble, trehalose (a naturally occurring osmolyte) was shown to stabilize the K1K2 peptide through preferential interaction. In addition, it was shown that the effect of denaturants such as GuHCl and stabilizing osmolytes such as trehalose is additive.⁶ Had the unfolded peptide displayed an ellipticity different than $\theta = 0$ mdeg at $\lambda = 215$ nm, the effect of trehalose would deviate from linearity in the presence of GuHCl. Our analysis showed that in fact the change in peptide stability as function of trehalose concentration remained linear in the presence of GuHCl, indicating that we have used the correct ellipticity of the unfolded ensemble at that wavelength.

Importantly, the limiting values for θ_{215} are applicable to all three peptide homologues due to their common isodichroic point. The reference spectra for the fully folded and fully unfolded ensembles are shown in Fig. S4. Also obtained is an estimate for the error in the values of the minimum, which was less than 10% of the signal.³ However, the errors reported in this work, estimated from the standard deviation of at least three repeat experiments make this error in the limiting value negligible.

b. CD spectra analysis of homologue peptides

The common isodichroic point and fully folded spectrum indicate the existence of the same two-state equilibrium for all peptides under all conditions. Specifically, both the folded (F) and unfolded (U) ensembles are the same for all homologues at all conditions, at least at the resolution detectable by the CD spectrometer.

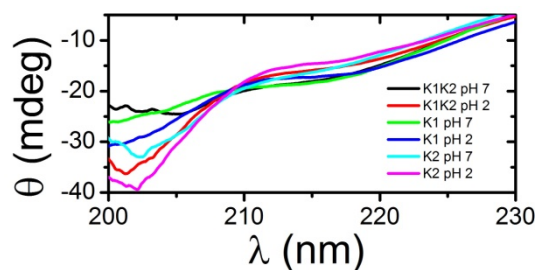


Figure S3. Circular dichroism spectra of all homologues at 100 μM and at two pH values. A single isodichroic point can be clearly seen at $\lambda = 208 \text{ nm}$.

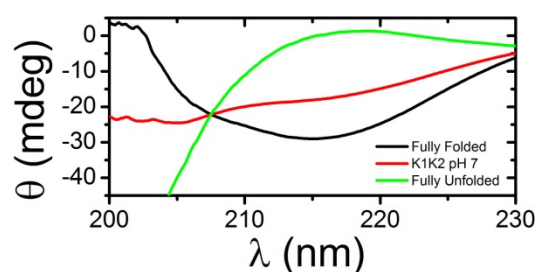


Figure S4. Reference spectra of folded and unfolded ensembles at 100 μM . The fully folded spectrum is obtained in a 1:1 volume ratio of methanol and water at 278 K, and shows the same isodichroic point at $\lambda = 208 \text{ nm}$. The fully unfolded spectrum is calculated from the spectrum of the K1K2 peptide at pH 7 and the fully folded spectrum, as previously shown.^{1,3} These spectra define the limiting values for θ_{215} . See SI Section 3a for more details.

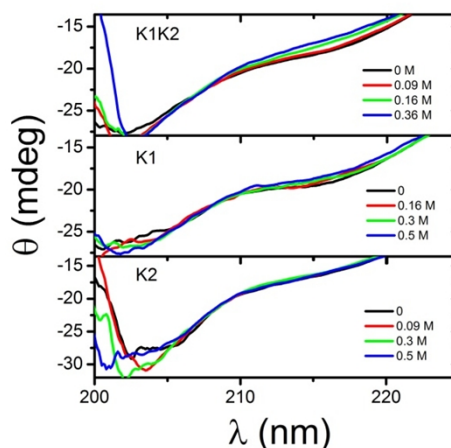


Figure S5. Selected CD spectra of salt titrations for all three homologues at 100 μM . The Isodichroic point is clearly visible at $\lambda = 208 \text{ nm}$.

Using the limiting values at $\lambda = 215 \text{ nm}$ for the folded ($\theta = -30.0 \text{ mdeg}$) and unfolded ($\theta = 0 \text{ mdeg}$, Fig. S4 and Section 3a), F and U populations for each

homologue and each condition were calculated and the equilibrium constant and subsequent free energy change upon folding were obtained through:

$$\Delta G = -RT \ln K = -RT \ln \left[\frac{\frac{\theta_{215}}{-30.0}}{1 - \left(\frac{\theta_{215}}{-30.0} \right)} \right]$$

Values for free energy of folding for different homologues and conditions are shown in Fig. S6. All free energies reported are averages from at least three independent measurements.

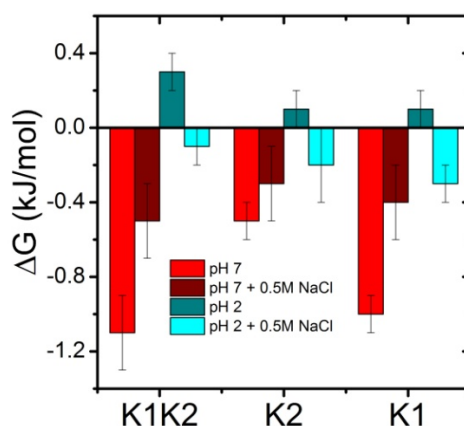


Figure S6. Folding free energy for all homologues at different conditions. Error bars are standard deviations from at least three repeats.

c. Fitting of ΔG_{salt}

The experimental values of ΔG_{salt} were fit to Eq. 1 to obtain the coefficients shown in Table S2 using OriginLab 8.6 (OriginLab, MA). The errors are standard errors obtained from the fit. For pH 2, the fit was a linear equation with the intercept fixed at the origin.

The values shown for m in Table S2 differ slightly in pH2 for the peptides K1 and K1K2. This is likely a result of a relatively strong destabilizing electrostatic effect (coefficient b) that remains an important factor even at the highest salt concentrations tested. The preferential interactions become dominant only at higher NaCl concentrations, and had we extended our measurements beyond 1.5 M, the value of m would have likely been higher, matching the slope of pH2 more closely. Unfortunately, due to sample aggregation we could not extend the reported concentration range.

Table S2. Fit parameters for Eq. 1.

	a (J/mol)	b (J/mol)	m (J/mol/mol _{NaCl})
K1	770 ± 50	160 ± 20	-450 ± 50
K2	300 ± 100	70 ± 30	-550 ± 90
K1K2	900 ± 40	220 ± 20	-450 ± 50
pH 2	0	0	-650 ± 70

d. Temperature dependence of ΔG

The temperature dependence of free energy changes provides the underlying entropic and enthalpic contributions via the Gibbs-Helmholtz relation:

$$\frac{\partial(\Delta G/T)}{\partial T} = -\frac{\Delta H}{T^2}$$

Fig. S7 A shows ΔG for all homologues at pH 7 (full symbols) and pH 2 (hollow symbols). The free energy derived from the equilibrium constant α is shown for all homologues in Fig. S7 B. While ΔG has a significant enthalpic contribution as implied by the slope, both K1K2 and K1 (and to a lesser extent K2) peptides show an almost constant value for ΔG_α , implying that there is little change in enthalpy upon SB formation, and that the free energy changes are related to entropy only.

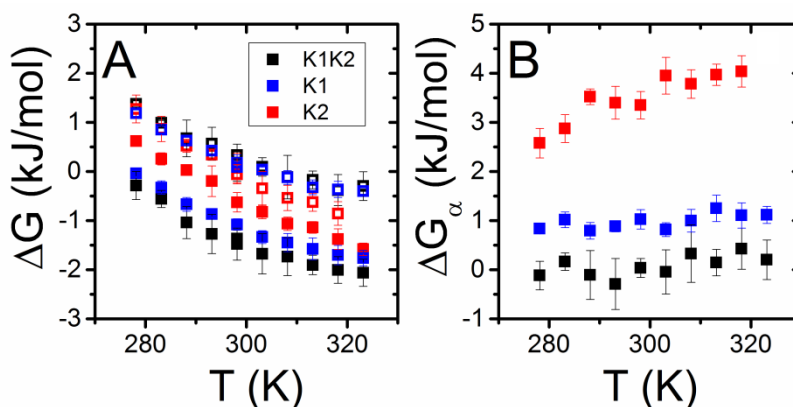


Figure S7. Temperature dependence of (A) folding free energy for different homologue, and (B) SB formation free energy ΔG_α , as defined in the main text.

e. Extent of ion release in salt-bridge formation

Free energy changes for salt-bridge formation as a function of salt allows the determination of the amount of previously bound counter-ions that are released into solution upon SB formation. Specifically, Record and co-workers showed that:⁷

$$\left(\frac{\partial \ln \alpha}{\partial \ln C_{\text{salt}}} \right) = \Delta v$$

Where Δv is the number of ion pairs released upon salt-bridge formation. Fig. S8 shows $\ln \alpha$, calculated from the interpolated values of the fit shown in Fig. 2 for each homologue. At low salt concentrations the curves are linear, a hallmark of the counter-ion release mechanism.⁷ As salt concentrations increase, and preferential interactions become dominant, the linear trend is lost. The slope for each homologue is shown in Table S3, and indicates the release of between 0.2 and 0.3 salt ion pairs per SB formed. This is unexpected since for the formation of a single salt-bridge one ion pair should be released from the charged moieties to the bulk solution. However, salt dependent changes occurring in the peptide backbone or the surrounding solvent may mitigate the apparent value of this release, reducing the value below the expected release of a single ion pair per SB.

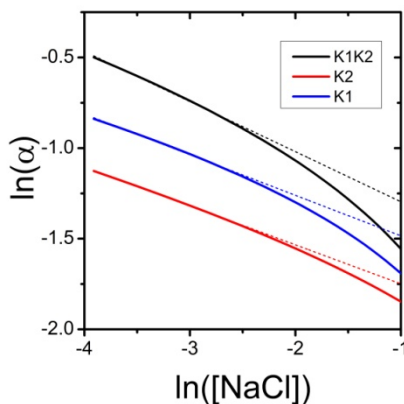


Figure S8. Salt concentration dependence of the equilibrium constant for salt-bridge formation. Dotted lines are linear fits of the extrapolated data shown in Fig. 2 in the main text.

Table S3. Extent of ion release upon SB formation

Homologue	Δv
K1K2	-0.28 ± 0.02
K1	-0.22 ± 0.01
K2	-0.22 ± 0.01

f. Distance distributions of opposite charges in the U ensemble.

An unfolded ensemble was generated using all-atom MD simulation of the extended peptide as previously reported.⁸ Briefly, simulations were performed using the NAMD simulation suite,⁹ using CHARMM27 forcefield with TIP3P water. Simulation boxes were run at 298K and 1 bar using Langevin thermostat and Nose-Hoover barostat algorithms. A production of 50 ns was derived from an initial extended conformation that was obtained from simulations at 400 K. From this, only the last 15 ns were taken for analysis. This ensemble was previously used to qualitatively predict the effect of various salts on the K1K2 peptide.¹⁰ To define salt-bridges, Kumar and Nussinov,¹¹ as well as other researchers,^{12,13} previously selected a cutoff of 4 Å between the center of mass of oppositely charged group ($-OOH^-$ or $-NH_3^+$) in crystal structures. We use a more lenient cutoff of 6 Å between groups. We determine the minimal opposite-charge distance in each frame in the trajectory. This distance can be due to any lysine (positions 1, 2, 10, or 11) interacting with the CT, as shown in Fig. S9 for each positive charge. The cumulative distribution probability is shown as a dashed magenta line (Right y-axis, Fig. S9). Less than 3% of the generated U ensemble fulfills this criterion for any of the charges.

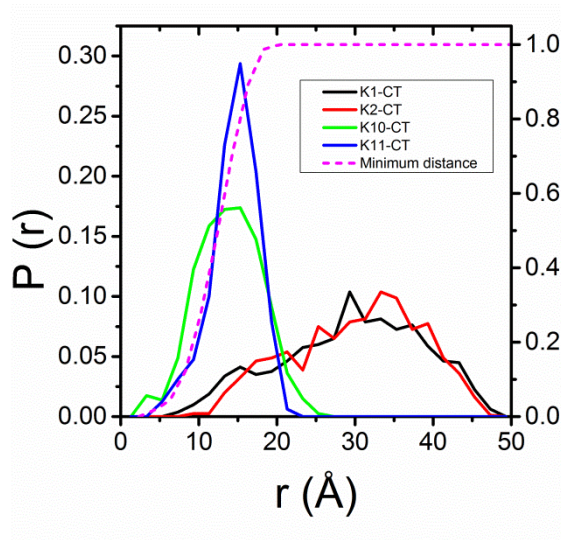


Figure S9. Probability for finding opposite charge distances in the unfolded ensemble from MD simulation. The right hand y-axis shows the cumulative probability of the minimal charge-charge distance (dashed magenta curve).

References

1. A. J. Maynard, G. J. Sharman, and M. S. Searle, *J. Am. Chem. Soc.*, 1998, **120**, 1996–2007.
2. M. S. Searle, S. R. Griffiths-Jones, and H. Skinner-Smith, *J. Am. Chem. Soc.*, 1999, **121**, 11615–11620.
3. R. Politi and D. Harries, *Chem. Commun.*, 2010, **46**, 6449–51.
4. B. Ciani, M. Jourdan, and M. S. Searle, *J. Am. Chem. Soc.*, 2003, **125**, 9038–47.
5. K. Wüthrich, *NMR of proteins and nucleic acids*, Wiley, 1986.
6. D. Harries and J. Rosgen, *Methods Cell Biol.*, 2008, **84**, 679–735.
7. M. T. Record Jr, C. F. Anderson, and T. M. Lohman, *Q. Rev. Biophys.*, 1978, **11**, 103–178.
8. R. Gilman-Politi and D. Harries, *J. Chem. Theory Comput.*, 2011, 3816–3828.
9. J. C. Phillips, R. Braun, W. Wang, J. Gumbart, E. Tajkhorshid, E. Villa, C. Chipot, R. D. Skeel, L. Kalé, and K. Schulten, *J. Comput. Chem.*, 2005, **26**, 1781–1802.
10. S. Sukenik, L. Sapir, R. Gilman-Politi, and D. Harries, *Faraday Discuss.*, 2013, **160**, 225.
11. S. Kumar and R. Nussinov, *ChemBioChem*, 2002, 604–617.
12. H. Gong and K. F. Freed, *Biophys. J.*, 2010, **98**, 470–7.
13. G. I. Makhatadze, V. V. Loladze, D. N. Ermolenko, X. Chen, and S. T. Thomas, *J. Mol. Biol.*, 2003, **327**, 1135–1148.